Energy loss of correlated ions in plasmas: Collective and individual contributions

E. M. Bringa and N. R. Arista
Centro Atómico Bariloche and Instituto Balseiro, Comisión Nacional de Energía Atómica, 8400 Bariloche, Argentina
(Received 27 November 1995; revised manuscript received 13 May 1996)

Interference effects in the energy loss of correlated ions in plasmas are studied using classical and quantum models for the dielectric response of the medium. The study covers the ranges of interest for inertial-confinement fusion, *Z* pinch, and Tokamak plasmas. The relative contributions from collective and individual excitations are evaluated, both for single and correlated ions. We derive analytical approximations for each of these terms. We find that collective excitations give a small contribution to the energy loss of single ions, for a wide range of plasma conditions, but produce the largest contribution to the interference effects for correlated ions. The differences of using classical or quantum cutoff parameters for the stopping and interference terms are analyzed. Numerical calculations of the interference effects for various cases, pertaining to the interaction of ion beams with fusion plasmas, are presented. [S1063-651X(96)01709-6]

PACS number(s): 52.40.Mj, 34.50.Bw

I. INTRODUCTION

One of the most relevant processes in the interaction between charged particles and plasmas is the phenomenon of the energy loss of the particles, due to localized collisions and excitation of collective modes in the plasma. In particular, this problem is of interest for current fusion research, like the heating of Tokamak plasmas with atomic beams [1], or the use of high-intensity ion beams as drivers for inertial-confinement fusion (ICF) studies [2,3]. Various aspects of this problem have received considerable attention.

On the other hand, the use of ion clusters has been proposed more recently, as an alternative mechanism to deposit a concentrated amount of energy in the medium. Earlier studies with molecular ions had shown that the energy loss of correlated ions in matter could in fact be enhanced, or diminished, by classical and quantum-mechanical interference effects [4,5]. The same mechanism was considered to be important in the case of very intense ion beams or ion clusters interacting with fusion plasmas [2,3].

The purpose of this work is to analyze in detail the energy loss of both single ions and correlated ions in plasmas of various densities and temperatures. The study is formulated in terms of the dielectric formalism for classical collisionless plasmas and includes calculations using also the quantum random-phase approximation (RPA). Collective and individual modes are taken into account in the spirit of the Bohm-Pines model [6,7], and the contribution of each mode is calculated. We develop analytical approximations for small and large velocities, and compare them with numerical calculations in cases of special interest.

In Sec. II we give a short review of the dielectric formalism, and of the main parameters of the problem. In Sec. III we consider the calculation of collective and individual contributions, and discuss several approximations. In Sec. IV we analyze the stopping of a dicluster, obtaining results for the interference effects and comparing with numerical integrations; we obtain analytical approximations and derive a simple scaling law for the interference function. The main conclusions of this work are summarized in Sec. VI.

II. FORMULATION AND PARAMETERS

The stopping power $S \equiv -dE/dx$ (energy loss per unit path length) of a point particle with charge Ze and velocity v, in a medium characterized by a dielectric function $\epsilon(k,\omega)$, in terms of the wave vector k and frequency ω, is given by [4,5,8]

$$S \equiv Z^2 S_0 = \frac{2(Ze)^2}{\pi v^2} \int_0^\infty \left(\frac{dk}{k}\right) \int_0^{kv} \omega \, d\omega \, \mathrm{Im}\left(\frac{-1}{\epsilon(k,\omega)}\right). \tag{1}$$

In the case of a classical plasma, the dielectric function can be conveniently parametrized as

$$\epsilon(k,\omega) = 1 + \left(\frac{k_D}{k}\right)^2 W(\zeta), \tag{2}$$

where $W(\zeta)$ is the plasma dispersion function [8], and

$$\zeta = \frac{(\omega + i\gamma)/\omega_P}{k/k_D}, \tag{3}$$

where we shall take the limit $\gamma \to 0$ for collisionless plasmas.

We introduce here some useful quantities: plasma frequency ω_P, thermal velocity v_T, Debye length λ_D, and wave number k_D, given as usual by

$$\omega_P^2 = \frac{4\pi n_P e^2}{m}, \quad v_T = \left(\frac{k_B T}{m}\right)^{1/2}, \quad \lambda_D = \left(\frac{v_T}{\omega_P}\right), \quad k_D = \lambda_D^{-1}, \tag{4}$$

where n_P is the plasma electron density and T is the electron temperature.

In the following, the stopping power expressions will be given in atomic units.

By separating the real and imaginary parts of $W(z) = X(z) + iY(z)$, we can write the stopping integral as follows:

$$S_0=\frac{2\omega_P^2}{\pi v^2}\int_0^\infty \frac{k^3dk}{k_D^4}\int_0^{v/v_T} z\,dz \times\left(\frac{Y(z)}{\left\{\left(\frac{k}{k_D}\right)^2+X(z)\right\}^2+[Y(z)]^2}\right) \quad (5)$$

in terms of the variable $z=\omega/kv_T$ $(0<z<v/v_T)$. Expressions for the functions $X(z)$ and $Y(z)$ are given in the Appendix.

To avoid logarithmic divergences in this integral for large k, a cut off $k_{\max}\equiv 1/b_{\min}$ must be introduced. The origin of this cutoff is due to the limit of applicability of the dielectric approach to treat short-range interactions $(b_{\min}<r<\lambda_D)$. In fact, there are two limiting values for $k_{\max}$ that should be considered: one from a classical and one from a quantum-mechanical origin. This question has been discussed in detail previously [9] using a description of short-range interactions based on quantum scattering theory, so that we give here only a brief discussion.

The quantum (perturbation theory) value is usually derived in the high-velocity limit of the Born approximation, where the value of $\hbar k$ represents the momentum transfer, and therefore $k_{\max}^{qm}=1/b_{\min}^{qm}\cong 2mv/\hbar$. The classical value arises from a treatment of close electron-ion collisions using a Coulomb potential, where the limiting value is the collision radius $b_{\min}^{cl}=Ze^2/mv^2$, which yields an upper limit to the wave vector: $k_{\max}^{cl}\cong 1/b_{\min}^{cl}$. The way these considerations can be generalized when the ion velocity is comparable (or smaller) than the mean electron velocity has been considered in Ref. [9]. We can summarize the results by the following limiting values:

Classical case $(\eta>1)$:

$$k_{\max}^{cl}\cong\frac{m}{|Z|e^2}\,(v^2+v_T^2). \quad (6)$$

Quantum case $(\eta<1)$:

$$k_{\max}^{qm}\cong\frac{2m}{\hbar}\,(v+v_T). \quad (7)$$

The parameter that indicates the applicability of the classical or quantum cases is the Bloch parameter η, defined by

$$\eta=\frac{k_{\max}^{qm}}{k_{\max}^{cl}}\cong\frac{|Z|e^2}{\hbar v_r}, \quad (8)$$

in terms of a relative velocity v_r given by $v_r^2=v^2+v_T^2$.

From these equations we can see that the $k_{\max}$ value to be used in Eq. (5) is always the smaller of both $k_{\max}^{cl}$ and $k_{\max}^{qm}$. The transition between both cases depends on the charge Z of the test particle, and the relative velocity v_r.

An important example is that of a slow test particle $(v\ll v_T)$, where one finds that the transition occurs at a plasma temperature [10]:

$$T_c\cong Z^2\times 10^6\ \text{K} \quad (9)$$

so that the classical collision regime is the one for $T<T_c$, and the quantum (perturbation) regime is that for $T>T_c$.

TABLE I. Some representative values of the main parameters for Tokamak, Z pinch, and ICF plasmas. The values of $b_{\max}$ have been calculated for typical velocities $v=1$, 7.5, and 35 a.u., respectively.

	Tokamak	Z pinch	ICF
n_P (1/cm^3)	10^{13}	10^{18}	3×10^{22}
ω_P (a.u.)	4.31×10^{-6}	1.36×10^{-3}	0.236
T (eV)	1000	20	300
v_T (a.u.)	6.06	0.857	3.32
λ_D (a.u.)	1.40×10^{6}	630	14.1
$b_{\max}$ (a.u.)	2.32×10^{5}	5.50×10^{3}	148
T/T_F	5.91×10^{8}	5.49×10^{3}	85.3

We note also that, due to the additional Z dependence of the classical cutoff value $k_{\max}^{cl}$ Eq. (6), the value of the stopping term S_0 in Eqs. (1) and (5) does not agree in general with the proton stopping power S_p. Only when the quantum $k_{\max}^{qm}$ value is used does S_0 become identical to S_p. The difference between both values may be specially significant for the case of highly charged ions.

The other important parameter in this problem is the length $b_{\max}$ representing the effective range of the interactions between the external particle and the electrons in the medium. The value of $b_{\max}$ depends on the particle velocity. At low velocities $(v<v_T)$ the interactions are very efficiently screened within a Debye distance, and so $b_{\max}$ is well represented by the Debye length $\lambda_D=v_T/\omega_P$. In the opposite case of high velocities $(v>v_T)$, the screening is modified by dynamical effects and the induced potential develops an oscillatory behavior behind the position of the moving ion (wake potential [11]). The effective range of the interactions in this case is given by the ''dynamical screening distance'' $b_{\max}=v/\omega_P$. The wavelength of the wake is related to $b_{\max}$ simply by $\lambda_{\text{wake}}=2\pi b_{\max}$.

To illustrate the ranges of interest for practical applications, we show in Table I some typical values of plasma densities and temperatures, and the corresponding values of λ_D and $b_{\max}$ (for ion velocities $v=1$, 7.5, and 35 a.u.), for the cases of Tokamak, Z pinch, and ICF plasmas.

In the following, the parameters shown in Table I will be taken as representative values, in order to estimate other quantities of interest for each case.

III. STOPPING POWER OF SINGLE IONS

The first problem to be considered now is the evaluation of the energy loss, using the dielectric formulation, for the simplest case of a single ion moving in the medium.

The calculation of the S_0 term can be handled in a convenient way by integrating first over the variable k in Eq. (5). Then, the problem reduces to evaluate a single integral over the variable $z=\omega/kv_T$, namely (cf. Refs. [8, 12])

$$S_0=\frac{2}{\pi}\left(\frac{\omega_P}{v}\right)^2\int_0^{v/v_T}dz\ zY(z)\left\{\ln\left(\frac{k_{\max}}{k_D}\right)+\frac{1}{4}\ln\left[\frac{\left(1+\frac{k_D^2}{k_{\max}^2}X(z)\right)^2+\left(\frac{k_D^2}{k_{\max}^2}Y(z)\right)^2}{[X(z)^2+Y(z)^2]}\right]-\frac{X(z)}{2Y(z)}\left[\arctan\left(\frac{k_{\max}^2/k_D^2+X(z)}{Y(z)}\right)-\arctan\left(\frac{X(z)}{Y(z)}\right)\right]\right\} \tag{10}$$

in terms of the functions $X(z)$ and $Y(z)$ given in the Appendix.

A. Individual and collective modes

The integrals in Eqs. (5) or (10) for S_0, can be separated in collective ($0<k<k_c$) and individual ($k_c<k<k_{\max}$) terms according to the Bohm and Pines theory [6,7]. The value of k_c separating both regimes is usually taken as the Debye constant $k_D\equiv 1/\lambda_D$.

The criterion to fix the value of k_c was studied in more detail from the properties of the dielectric function $\epsilon(k,\omega)$; a discussion of this point is given in the Appendix. In practice, since the values of the stopping integrals depend in a logarithmic way on k_c, the approximation $k_c\cong k_D$ can be considered satisfactory for the present calculations.

Therefore, we separate the collective and individual contributions in Eqs. (5) and (10) as follows:

$$S_0=\int_0^{k_D}f(k)dk+\int_{k_D}^{k_{\max}}f(k)dk=S_0^{\rm col}+S_0^{\rm ind}. \tag{11}$$

The calculation of the stopping power S_0 may be performed in a numerical way by integration using Eq. (5). However, for practical purposes it becomes useful to derive analytical approximations for the cases of high and low velocities.

1. High-velocity approximations ($v>v_T$)

The integrals in Eq. (11) may be evaluated analytically by using the approximations to the energy-loss function $\mathrm{Im}[-1/\epsilon(k,\omega)]$ given in the Appendix [Eqs. (A6) and (A8)].

In this way we obtain:

$$S_0=S_0^{\rm col}+S_0^{\rm ind}\simeq\left(\frac{\omega_P}{v}\right)^2\left[\ln\left(\frac{v}{v_T}\right)\Theta(v-v_T)+\ln\left(\frac{k_{\max}}{k_D}\right)\Theta(k_{\max}-k_D)F_1\left(\frac{v}{v_T}\right)\right], \tag{12}$$

where the first term is due to collective excitations and the second is due to individual excitations.

The function $F_1(x)$ is given by

$$F_1(x)=\left(\frac{2}{\pi}\right)^{1/2}\int_0^x z^2\exp\left(\frac{-z^2}{2}\right)dz, \tag{13}$$

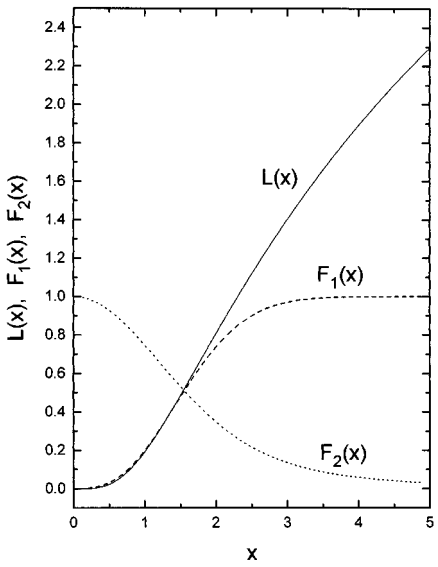

FIG. 1. Functions $L(x)$, $F_1(x)$, and $F_2(x)$, pertaining to the analytical approximations of the stopping and interference terms in Eqs. (12), (16), (30), and (35).

and it is shown in Fig. 1.

In the limiting case of $v/v_T\to\infty$, we get $F_1(v/v_T)\to 1$, and therefore

$$S_0=\left(\frac{\omega_P}{v}\right)^2\ln\left[\frac{k_{\max}}{k_{\min}}\right]; \tag{14}$$

where $k_{\min}=\omega_P/v=1/b_{\max}$ is a dynamical screening parameter that is determined by the dielectric model.

If the quantum-mechanical value of $k_{\max}\cong 2mv/\hbar$ is used one obtains the well-known Bethe expression for the collision logarithm: $\ln(2mv^2/\hbar\omega_P)$, whereas if the classical value of $k_{\max}\cong mv^2/|Z|e^2$ is used, one gets Bohr's expression: $\ln(mv^3/|Z|e^2\omega_P)$. The transition between both values may be described more accurately using the following expression derived from a transport cross-section approach [9] (more appropriate to describe close collisions)

$$\ln\left[\frac{k_{\max}}{k_{\min}}\right]\cong\ln\left[\frac{\alpha v^2}{(1+\beta v^2)^{1/2}}\right], \tag{15}$$

where $\alpha=1.123mv/Ze^2\omega_P$, $\beta=(\hbar/\Gamma Ze^2)^2$, and $\Gamma=1.781$. In general, a reasonably good approximation to $k_{\max}$ is obtained by always using the smallest of both $k_{\max}^{cl}$ and $k_{\max}^{qm}$ values. We note that the Z dependence introduced through the value of $k_{\max}$ could be important in the case of highly charged ions, when $Ze^2/\hbar v\geqslant 1$, and the stopping integral depends on $k_{\max}^{cl}\cong mv^2/|Z|e^2$.

2. Low-velocity approximations ($v<v_T$)

In this case, excitation of collective modes can not take place, so that we consider only short-range excitations. Then the approximation $z\ll 1$ to the dielectric function [see Appendix, Eq. (A7)] may be used.

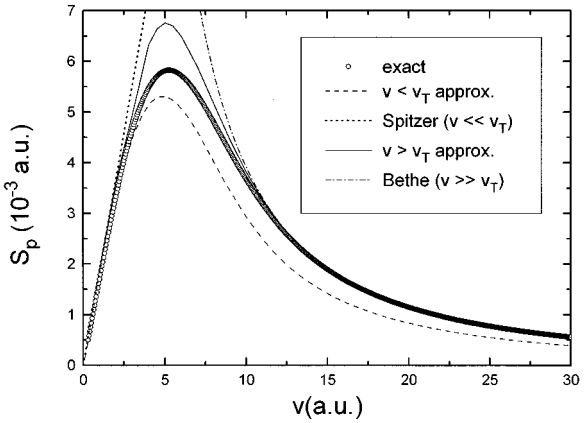

FIG. 2. Comparison between analytical approximations and exact integrations of stopping powers for protons. The circles show the exact results obtained by integration of Eq. (10). The dashed and solid lines show the high- and low-velocity approximations of Eqs. (12) and (16). The approximations for $v \ll v_T$ (Spitzer) and $v \gg v_T$ (Bethe) are also shown.

The stopping power can be approximated in this case as follows:

$$S_0 = \frac{1}{3}\left(\frac{2}{\pi}\right)^{1/2} \frac{1}{\lambda_D^2} L\left(\frac{k_{\max}}{k_D}\right)\left(\frac{v}{v_T}\right) F_2\left(\frac{v}{v_T}\right), \tag{16}$$

where $L(x)$ is the low-velocity collision logarithm

$$L(x) = \frac{1}{2}\left[\ln(1+x^2) - \frac{x^2}{(1+x^2)}\right] \tag{17}$$

and

$$F_2(x) = \frac{3}{x^3}\int_0^x z^2 \exp\left(\frac{-z^2}{2}\right) dz. \tag{18}$$

The functions $L(x)$ and $F_2(x)$ are shown in Fig. 1. In particular, we find the following limits: $F_2(x) \to 1$, when $x \to 0$, and $F_2(x) \to 0$, when $x \to \infty$.

For $v \ll v_T$, $k_{\max}$ does not depend on v, and the dependence of the stopping power with velocity is linear. A simple result in this limit was first obtained for classical plasmas by Spitzer [13], namely,

$$S_0 = \frac{4}{3}\sqrt{2\pi}\,\frac{nv}{(k_B T)^{3/2}} L\left(\frac{v_T^3}{Z\omega_P}\right). \tag{19}$$

This result is retrieved from Eq. (16) in the limit $v \ll v_T$.

The function $xF_2(x)$ in Eq. (16) generates a maximum in the stopping, similar to the high-velocity case of Eq. (12).

B. Results of numerical integrations

We show in Fig. 2 the values of the stopping power for protons S_p, in an ICF plasma, as calculated by the numerical integration of Eq. (10) (considered here as the exact values), and using the approximations discussed before. The $v > v_T$ and $v < v_T$ approximations are those given by Eqs. (12) and (16); they provide useful upper and lower estimations to the exact values in the whole range of velocities.

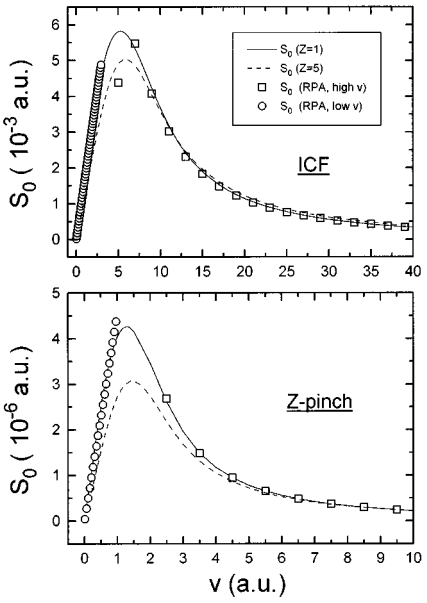

FIG. 3. Calculations of the stopping power term S_0 in Eqs. (1) and (5) for ICF and Z-pinch plasmas, using the parameters from Table I. The solid lines show calculations for protons using the classical dielectric formulation with a quantum value for $k_{\max}$; the dashed lines show calculations for ions with effective charge $Z=5$ using the classical value of $k_{\max}$. The symbols show the results of the quantum RPA calculations for low and high velocities.

The typical behavior of the stopping with velocity is appreciated: a linear velocity dependence for $v < v_T$ (Spitzer regime), a maximum at $v_{\max} \sim 2v_T$, and a nearly quadratic decrease with velocity for $v > v_T$ (Bethe regime). A characteristic value for the stopping power is given by the value at the maximum

$$S_{\max} \sim \left(\frac{Ze\omega_P}{v_T}\right)^2 \sim c_s \frac{4\pi Z^2 e^4 n_P}{k_B T}, \tag{20}$$

where the coefficient c_s varies weakly with density and temperature (its value ranges between 0.8 and 2.5 for all the cases studied here).

It is of interest to compare the present results, using a classical dielectric function (CDF), with those calculated using the quantum random-phase approximation (RPA) [14–16]. The CDF and RPA results nearly coincide for large T/T_F (where $T_F = E_F/k_B$ is the Fermi temperature) if one uses the quantum value of $k_{\max}$ from Eq. (7). Figure 3 shows the RPA results for $v \ll v_T$ and $v \gg v_T$, according to Ref. [16], for the typical ICF and Z-pinch cases. The CDF and RPA results for protons agree very well for these cases of weak electronic degeneracy. However, the results for $Z=5$, where the classical value of $k_{\max}$ must be used, show a significant difference with the quantum calculations.

C. Analysis of collective and individual terms

In Fig. 4 we show the results of separate calculations of the collective and individual contributions to the stopping power for protons, as well as the total stopping, for different plasma conditions. In each case, the exact calculations are compared with the analytical high-velocity approximations.

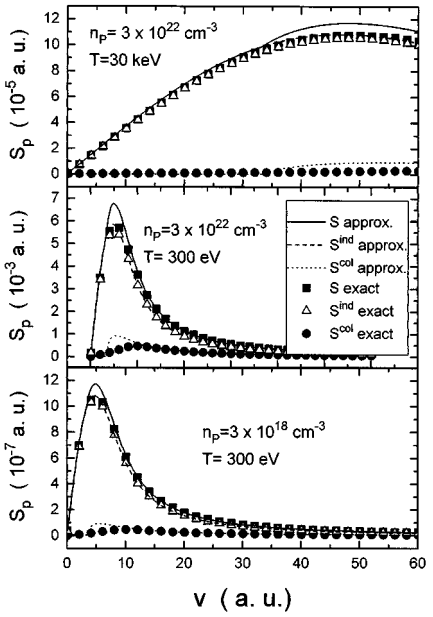

FIG. 4. Collective and individual contributions to the stopping power for protons in plasmas of various densities and temperatures. The solid symbols show the exact values obtained by numerical integration; the lines show the corresponding approximations, as indicated in the inset.

The simple approximation for the collective modes (dotted lines) produces larger stopping values near the maximum, as compared with the exact results, but the effect on the total values is not very significant.

To illustrate more generally the relative significance of collective and individual contributions to the stopping of uncorrelated particles, we plot the lines in Fig. 5, in the $n_P - T$ plane, corresponding to constant values of the ratio

$$\frac{S^{\mathrm{col}}}{S^{\mathrm{ind}}} \simeq \frac{\ln(b_{\max}/\lambda_D)}{\ln(\lambda_D/b_{\min})} \frac{1}{F_2(v/v_T)} \simeq \frac{\ln(b_{\max}/\lambda_D)}{\ln(\lambda_D/b_{\min})}, \quad (21)$$

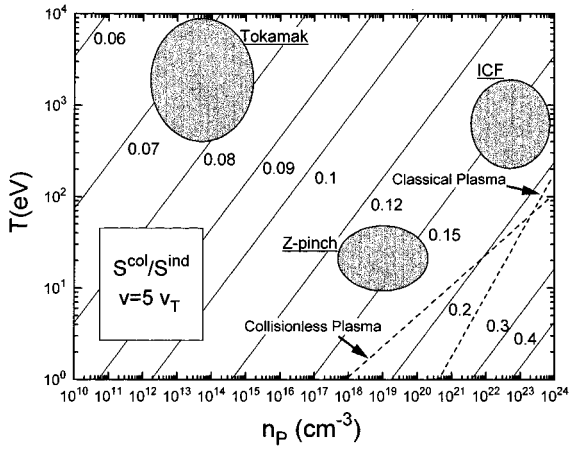

FIG. 5. Study of the relative contribution of collective and individual modes to the proton stopping power, for wide ranges of plasma densities and temperatures, including the ranges of ICF, Z pinch, and Tokamak plasmas. The individual type of interactions are shown to be the dominant mechanism of energy loss through the whole range of interest.

(where $b_{\max}=v/\omega_P$ and $b_{\min}=1/k_{\max}$), for a particle with velocity $v=5v_T$.

In general, we see from Eq. (21) that the contribution from individual modes will be greater than that from collective modes if

$$\Gamma \equiv b_{\max} b_{\min}/\lambda_D^2 \ll 1. \quad (22)$$

It can be seen that the importance of collective effects increases with plasma density and decreases with temperature, being relatively more important for the case of ICF plasmas (as is well known, collective terms play a very important role in solid-state plasmas [17]).

This behavior may be simply explained as follows: temperature increase the ratio between average kinetic energy and interaction energy of the plasma particles. This shifts the value of λ_D and then the individual terms increase with respect to the collective ones.

As a corollary, this produces a significant departure from Bohr's *equipartition rule*, which states nearly equal contributions from collective and individual stopping terms. This rule applies to the stopping of particles in solids or in other dense media. As can be observed from Fig. 5 the contribution from individual collision terms becomes the dominant mode of energy loss for the case of single (or uncorrelated) ions, through the whole range of plasma parameters of interest.

IV. STOPPING OF A DICLUSTER

The energy loss of a pair of charges in correlated motion (a *dicluster*) shows some significant differences with the case of uncorrelated particles discussed before. These differences come from interference effects in the simultaneous interactions of both particles with the medium [4,5]. For the range of parameters previously considered, and internuclear distances of several atomic units, the interferences are generally more important for the collective-interaction terms, than for the individual ones. Therefore, the role of collective terms in this case must be carefully reevaluated.

Let us consider now the interference effects in the energy loss of a dicluster, formed by two particles in motion through the plasma with velocity $\vec{v}$ and internuclear distance $\vec{r}$. We will assume that both particles have equal charges $Z_1=Z_2=Z$.

Using the previous formulation, and following Ref. [4], the stopping power of a dicluster can be expressed as follows:

$$S_{\mathrm{dicl}} = 2Z^2[S_0 + I(\vec{r})] \quad (23)$$

in terms of the stopping power S_0, defined in Eqs. (1) and (5), and with the interference function $I(\vec{r})$ given by [4]

$$I(\vec{r}) = \left(\frac{1}{2\pi^2 v}\right) \int d\vec{k} \left(\frac{\vec{k}\cdot\vec{v}}{k^2}\right) \mathrm{Im}\left(\frac{-1}{\epsilon(k,\omega)}\right) \cos(\vec{k}\cdot\vec{r}). \quad (24)$$

The expected limits of the function $I(\vec{r})$ and of the dicluster stopping are the following:

(i) for $r\to 0$: $I(\vec{r})\to S_0$,

and $S_{cl}\to(2Z)^2 S_0$ (one particle of charge $2Z$),

(ii) for $r\to\infty$: $I(\vec{r})\to 0$, and $S_{cl}\to 2(Z^2 S_0)$

(two independent particles of charge Z). (25)

In the usual experimental situations the incident diclusters are randomly oriented, so that one must take the average of the interference term with respect to the angle θ between $\vec{r}$ and $\vec{v}$. In this case one obtains

$$I(r)=\left(\frac{2}{\pi v^2}\right)\int_0^\infty \frac{dk}{k}\left(\frac{\sin(kr)}{kr}\right)\int_0^{kv}\omega\, d\omega\ \mathrm{Im}\left(\frac{-1}{\epsilon(k,\omega)}\right). \tag{26}$$

The case where the dicluster is oriented parallel to the direction of motion has been studied previously by D'Avanzo, Lontano, and Bortignon [18]. More recently, orientational effects have also been studied [19]. These effects may become important for longer time scales than those usually considered in ICF studies [3] (for instance, they could be important in the case of particle clusters injected in Tokamaks). In the following calculations, orientational effects will be neglected.

Using the dielectric function for a classical collisionless plasma Eq. (2) one can write the integral for the interference term $I(r)$ as follows:

$$I(r)=\frac{2\omega_P^2}{\pi v^2}\int_0^\infty \frac{k^3 dk}{k_D^4}\left(\frac{\sin(kr)}{kr}\right)\int_0^{v/v_T} z\, dz \times\left(\frac{Y(z)}{\left\{\left(\frac{k}{k_D}\right)^2+X(z)\right\}^2+[Y(z)]^2}\right). \tag{27}$$

The integration over the k variable may be performed analytically. After some algebra, one can express the function $I(r)$ as a single integral

$$I(r)=\frac{2}{\pi}\left(\frac{\omega_P}{v}\right)^2\left(\frac{\lambda_D}{r}\right)\int_0^{v/v_T} z\, dz\ \mathrm{Im}[F(z,k_{\max},r)], \tag{28}$$

where

$$F(z,k_{\max},r)=q\{\sin(qr)[\mathrm{Ci}((k_{\max}-q)r)+\mathrm{Ci}((k_{\max}+q)r) -\mathrm{Ci}(-qr)-\mathrm{Ci}(qr)]+\cos(qr) \times[\mathrm{Si}((k_{\max}-q)r)-\mathrm{Si}((k_{\max}+q)r) -2\mathrm{Si}(-qr)]\}, \tag{29}$$

with $q\equiv q(z)=k_D\sqrt{X(z)+iY(z)}$, and where $\mathrm{Si}(x)$ and $\mathrm{Ci}(x)$ denote the sine and cosine integrals [20]. We will now obtain approximate analytical results for the interference term $I(r)$ in Eq. (28).

(a) *High-velocity approximations*. Using similar approximations to those considered in the preceding section, for the case of ions with velocities $v\gg v_T$, we can separate the contributions from individual and collective modes, so that the integral $I(r)$ can be approximated by

$$I(r)\simeq\left(\frac{\omega_P}{v}\right)^2\left[I_1\left(\frac{\omega_P r}{v},\frac{r}{\lambda_D}\right)\theta(v-v_T) +F_1\left(\frac{v}{v_T}\right)I_1\left(\frac{r}{\lambda_D},k_{\max}r\right)\theta(k_{\max}-k_D)\right] =I^{\mathrm{col}}(r)+I^{\mathrm{ind}}(r), \tag{30}$$

where $F_1(v/v_T)$ is the same function that appears in the high-velocity stopping power formula Eq. (13) and

$$I_1(x,y)=\int_x^y\left(\frac{\sin(z)}{z^2}\right)dz=H(x)-H(y), \tag{31}$$

with $H(x)$ defined by

$$H(x)=\left(\frac{\sin(x)}{x}\right)-\mathrm{Ci}(x). \tag{32}$$

For $v\gg v_T$ ($x\gg 1$), $F1(x)\cong 1$, and we get

$$I(r)\cong k_{\min}^2\, I_1(k_{\min}r,k_{\max}r), \tag{33}$$

where $k_{\min}\equiv 1/b_{\max}=\omega_P/v$. Therefore, the functional dependence of the interference function in this approximation, in terms of the beam-plasma parameters, is given only through $k_{\min}r$ and $k_{\max}r$.

For large r ($k_{\max}r\gg 1$), the term with $k_{\max}$ in Eq. (33) can be neglected. This corresponds to the limit where the internuclear distance is sufficiently large with respect to the minimum electron-ion distance of approach in closest collisions, so that the two ions behave as independent scattering centers for this type of short-range collisions.

In this case, $I(r)$ can be further approximated as

$$I(r)\simeq\left(\frac{1}{b_{\max}}\right)^2\left[\frac{\cos(r/b_{\max})}{(r/b_{\max})^2}\right]. \tag{34}$$

Since $b_{\max}=v/\omega_P$, we find that the temperature dependence if $I(r)$ disappears in this limit. The relevant parameter here becomes the ratio between the internuclear distance r, and the wavelength of the wake potential: $\lambda_{\mathrm{wake}}=2\pi b_{\max}=2\pi v/\omega_P$. This represents the interferences between the wakes produced by each of the two particles, which are separated by the distance r.

(b) *Low-velocity approximations*. Using now the approximation $z\ll 1$ (see Appendix) for the case of ions with velocities $v\ll v_T$, and integrating Eq. (27), we get for the dicluster a low-velocity approximation to the interference term, namely,

$$I(r)=\left(\frac{2}{\pi}\right)^{1/2}\frac{1}{3\lambda_D^2}\,I_2(r/\lambda_D,k_{\max}/k_D)\left(\frac{v}{v_T}\right)F_2(v/v_T), \tag{35}$$

where $F_2(x)$ has been defined before [Eq. (18)] and

$$I_2(x,y)=\int_0^y dz\ z^3\left(\frac{\sin(zx)}{zx}\right)(1+z^2)^{-2}, \tag{36}$$

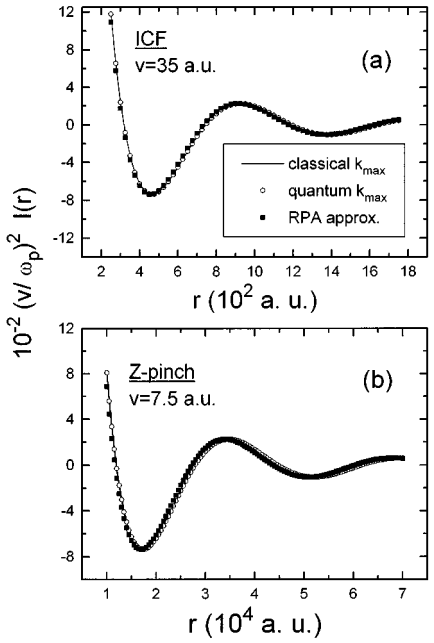

FIG. 6. Calculation of the interference term $I(r)$ for the cases of ICF and Z-pinch plasmas, using the values from Table I. The calculations from Eq. (28), using the classical dielectric function, and using both classical and quantum values of $k_{\max}$ [Eqs. (6) and (7)] are compared with the quantum dielectric formulation arising from the random-phase approximation.

(I_2 can be solved in term of special functions, but a numerical evaluation is easier).

Comparison of Eqs. (35) and (16) shows that in this limit the interference effects can be parametrized as follows: $I(r)/S_0 = I_2(x,y)/L(y)$, with $x = r/\lambda_D$, and $y = k_{\max}/k_D$.

In this case, the response of the plasma to the moving particles is nearly static, and the dicluster ions are screened by the plasma electrons according to Debye potentials. Hence, interference effects will be important for separations r shorter than λ_D. The united-ions limit: $I(r)/S_0 \cong 1$, will be obtained for very small distances, $r < b_{\min} = 1/k_{\max}$ [with $k_{\max}$ given by Eqs. (6) and (7) in the limit $v \ll v_T$].

A. Results of calculations

Calculations have been performed using the exact integral expressions provided by the dielectric formulation. We have used both a classical dielectric function and a quantum RPA treatment [14–16]. We analyze here the dependence of the interference term on the ion distance r, and on the dicluster velocity v.

1. High velocities

The behavior of the interference term I is shown in Fig. 6, for conditions corresponding to (a) ICF and (b) Z-pinch plasmas. The interference term has been multiplied by the factor $(v/\omega_P)^2$ in order to show similar scales in the ordinate axis; we note however the very different scales (between the Z-pinch and the ICF cases) in the abscissa values. The similar shapes of the results in both cases—(a) and (b)—suggest the existence of a simple scaling rule, a point that will be analyzed below. The figures show a very good agreement between these results, using either a classical or a quantum value of $k_{\max}$.

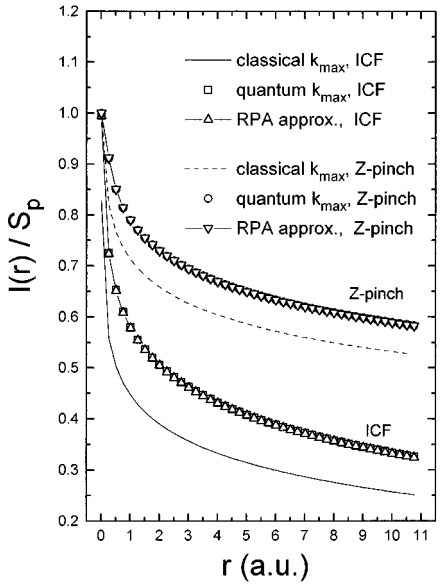

FIG. 7. Ratios $I(r)/S_0$, between the interference and the stopping terms, obtained from the integrations of Eqs. (28) and (10), for the ICF and Z-pinch cases of Table I. The calculations using a classical and a quantum cutoff value for $k_{\max}$ are compared with similar integrations using the RPA dielectric function.

The ratio $I(r)/S_0$, between the interference and the stopping terms, is shown in Fig. 7, for large velocities and small values of r. Here we find important differences between the classical and the quantum choices of $b_{\min} \equiv 1/k_{\max}$. This difference is produced by the dependence (on $k_{\max}$) of the stopping term S_0 alone; i.e., the dependence of $I(r)$ on $k_{\max}$ is negligible (Fig. 6), except for very small distances ($r \sim b_{\min}$) not shown here.

We find in these cases an excellent agreement with the RPA results, provided that in the calculation of the stopping term S_0 the quantum value of $k_{\max}^{qm} = 2mv/\hbar$ [from Eq. (7)] is used [which in these examples is the correct value according to the Bloch criterion Eq. (8), since $\eta < 1$ in the high-velocity range]. Moreover, since Bloch criterion yields always the smallest value of $k_{\max}$—and hence the smallest S_0—the ratio $I(r)/S_0$ is always maximized.

2. Low velocities

For low velocities and large r values (respect to λ_D), $I(r)$ tends quickly to zero, and it shows no oscillatory behavior for very large distances. The difference between the classical and the quantum cases becomes here more relevant, as shown in Fig. 8, for $Z=5$ in a dense plasma. The present calculation coincides with the RPA results [14–16] when the quantum value of $k_{\max}$ is used. However, we should note that in this case ($\eta > 1$) the correct cutoff is given by the classical value $k_{\max}^{cl} = k_B T/|Z|e^2$ [from Eq. (6)], which now yields much larger values for the ratio $I(r)/S_0$, as shown in Fig. 8(b).

B. Collective and individual contributions

In the range of high velocities $v > v_T$ the energy loss is partitioned in individual and collective excitations. As dis-

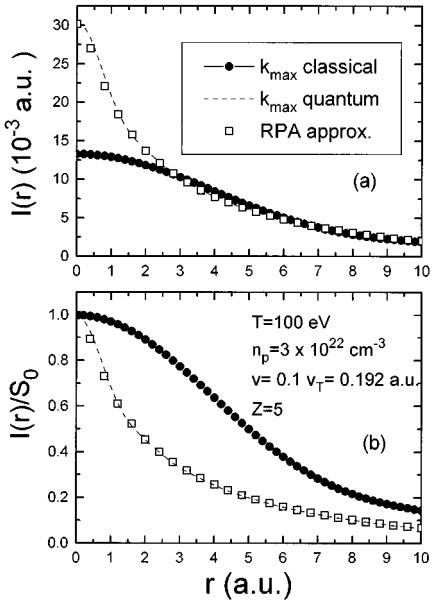

FIG. 8. Calculations of the interference term $I(r)$ [part (a)], and ratios $I(r)/S_0$ [part (b)], in the low-velocity range ($v=0.1v_T$), vs internuclear distance r, for correlated ions with charge $Z=5$. The RPA results agree with those obtained using a quantum cutoff value for $k_{\max}$, but the correct results in this case are those corresponding to the classical cutoff values [Eq. (6)], shown by solid circles.

cussed before (cf. Fig. 5), the contribution of collective modes represents usually a small fraction of the stopping term S. However, in the integration of the interference term I the contribution of collective modes becomes very important. We show in Fig. 9 the separate contributions from each mode, $I_{\rm col}$ and $I_{\rm ind}$, for internuclear distances $r=100$ and 5000 a.u. We find that the contribution of collective modes becomes most important for large internuclear distances. In

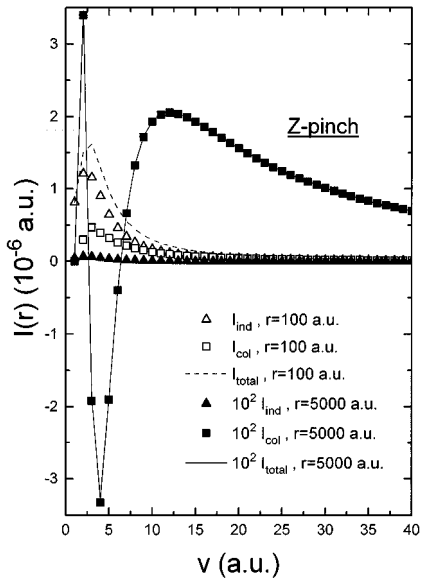

FIG. 9. Collective and individual contributions to the interference term $I(r)$ for internuclear distances $r=100$ and 5000 a.u., as a function of velocity. The collective contribution becomes dominant for the largest distance.

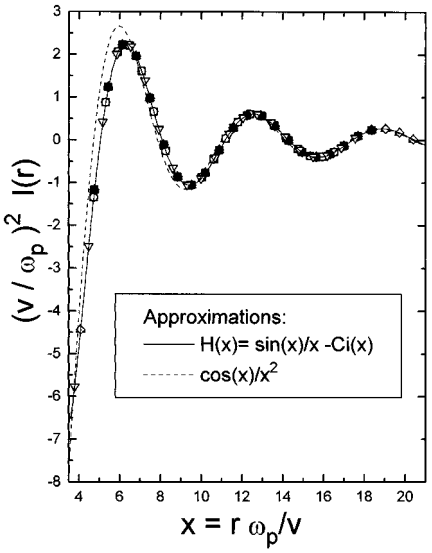

FIG. 10. Scaling of the interference term $I(r)$, as predicted by the high-velocity approximation of Eq. (38), using the results of numerical integrations of Eq. (28), for ICF, Z pinch and Tokamak plasmas.

particular, the interference effect for $r=5000$ a.u. is completely dominated by collective modes.

C. Scaling of the interference function

Let us finally consider a simple scaling property of the interference function $I(r)$ in the limit of high velocities. According to Eqs. (31) and (33), with $b_{\max}=v/\omega_P$

$$I(r)=\left(\frac{\omega_P}{v}\right)^2\left[H\left(\frac{r\omega_P}{v}\right)-H\left(\frac{r}{b_{\min}}\right)\right]. \tag{37}$$

Due to the rapid decay of the function $H(x)$ for $x\gg 1$, Eq. (32), in many cases we can neglect the second term $H(r/b_{\min})$ in Eq. (37) (this is particularly true for swift atomic clusters, where the values of r are of the order of a few atomic units—or much larger if Coulomb explosion is considered,—while the values of both $b_{\min}^{qm}\approx\hbar/2mv$ and $b_{\min}^{cl}\approx Ze^2/mv^2$ decrease with velocity). Therefore, we can approximate $I(r)$ in the limit $r\gg b_{\min}$, by

$$I(r)\cong\left(\frac{\omega_P}{v}\right)^2 H\left(\frac{r\omega_P}{v}\right). \tag{38}$$

To illustrate this relation, we show in Fig. 10 a set of calculated values of $(v/\omega_P)^2 I(r)$, for different beam and plasma parameters, including ICF, Z pinch, and Tokamak plasmas. The values are rescaled in terms of the variable $x=r\omega_P/v$. The simple (asymptotic) approximation: $H(x)\approx\cos(x)/x^2$ gives also very good results in this range of x values. Therefore, we can now explain the similarity noted earlier, between Figs. 6(a) and 6(b), as a consequence of this scaling property.

The physical content of this property should be clear from the previous discussions. For high velocities, the main scale of distance is the characteristic length of the wake $\lambda_{\rm wake}=2\pi v/\omega_P$. Therefore, the ions interact appreciably

only at distances shorter than λ_{wake}, and hence the interference function scales in a general way with the parameter $2\pi r/\lambda_{wake}=r\omega_P/v$.

V. SUMMARY AND CONCLUSIONS

The energy loss of single and correlated ions in plasmas has been studied both numerically and analytically for various plasma conditions, showing in detail the influence of the most relevant parameters. The use of a classical dielectric function allows a simple integration of the stopping power and interference terms. When the quantum cutoff value of k_{max} is used in the dielectric formulation the results agree very well with those obtained from the RPA model.

The use of a classical cutoff value (k_{max}^{cl}) in the integrals becomes more appropriate in the case of highly charged ions at low velocities. Important differences may result from the use of inadequate values of k_{max}, specially in the evaluation of the stopping terms.

The contributions arising from individual and collective plasma modes were analyzed in detail. A more general study of the collective resonances, as emerging from the classical dielectric function, is included in the Appendix. Other conclusions of interest for the cases of single and correlated ions are the following:

(a) *Single ions*. The separation of the energy loss in terms of collective and individual modes was studied and previous approximations were analyzed. We conclude that for a wide range of plasma conditions, including the cases of ICF, *Z* pinch, and Tokamak plasmas, the energy loss is dominated by individual-collision terms. Therefore, Bohr's equipartition rule does not hold for the stopping power of nondegenerate plasmas. In general, the contribution of collective modes increases with plasma density, and decreases with temperature.

We find that the contribution from individual modes is greater than the one from collective modes if

$$\Gamma \equiv b_{max} b_{min}/\lambda_D^2 \ll 1, \tag{39}$$

where $b_{max}=v/\omega_P$ and $b_{min}=1/k_{max}$. This justifies the use of kinetic-type formulations [9] when $\Gamma \ll 1$, because collective modes can be neglected.

(b) *Correlated ions*. In the low-velocity case, the interference effects are important only if the distances between both ions is similar to, or smaller than, the Debye length λ_D. This condition is satisfied very well in the case of molecular ions injected in plasmas (for the three cases of Tokamak, *Z* pinch, and ICF plasmas considered here).

For high velocities, the interference function scales in a general way with the parameter $r\omega_P/v$. Since the value of b_{max} increases with velocity, the interference effects will become more important, and one can expect large collective effects not only for clusters of ions, but also in some conditions, for very intense ion beams.

The scaling properties of the interference effects and the analytical approximations derived here may be useful to study the collective effects in the energy loss of large ion clusters [21]. Further calculations along these lines will be reported in a separate paper.

ACKNOWLEDGMENTS

This work was partially supported by Consejo Nacional de Investigaciones Científicas y Técnicas, (Argentina), through a research grant (PID No. 300192) and a research Fellowship awarded to E.M.B.

APPENDIX

In this appendix we summarize some properties of the dielectric function of classical plasmas and discuss in more detail the separation of collective and individual modes.

1. Dielectric function for a classical plasma

Following the usual approach [7,8], the longitudinal dielectric function $\epsilon(k,\omega)$ is given by

$$\epsilon(k,\omega)=1+\left(\frac{4\pi e^2}{k^2}\right)\int d\vec{v_e}\left(\frac{\vec{v_e}\cdot\vec{k}}{\omega-\vec{v_e}\cdot\vec{k}+i\gamma}\right)\left(\frac{\partial f_0}{\partial E_e}\right), \tag{A1}$$

where $E_e=mv_e^2/2$ and $f_0=f_0(\vec{v_e})$ is the Maxwell-Boltzmann distribution of electrons velocities $\vec{v_e}$. Using the parameters ω_P, v_T, λ_D, and k_D from Eq. (4) one finds [7]

$$\epsilon(k,\omega)=1+\left(\frac{k_D}{k}\right)^2 W\left(\frac{(\omega+i\gamma)/\omega_p}{k/k_D}\right). \tag{A2}$$

For $\gamma\to 0$ (collisionless plasma) the function $W(z)$ can be expressed, in terms of the variable $z=\omega/kv_T$, as follows:

$$W(z)=X(z)+iY(z), \tag{A3}$$

with

$$X(z)=1-z\ \exp\left(\frac{-z^2}{2}\right)\int_0^z dx\ \exp\left(\frac{x^2}{2}\right), \tag{A4}$$

and

$$Y(z)=\left(\frac{\pi}{2}\right)^{1/2} z\ \exp\left(\frac{-z^2}{2}\right). \tag{A5}$$

2. Approximations for $\epsilon(k,\omega)$

In order to obtain analytical approximations for the energy loss and interference terms, simple expressions for the energy-loss function $\mathrm{Im}[-1/\epsilon(k,\omega)]$ become useful.

Using the variable $z=\omega/kv_T$, the limits of interest are the following:

(a) for $z\gg 1$:

$$\mathrm{Im}\left(\frac{-1}{\epsilon(k,\omega)}\right)\cong\frac{\pi}{2}\,\omega_P[\,\delta(\omega-\omega_P)-\delta(\omega+\omega_P)]; \tag{A6}$$

(b) for $z\ll 1$:

$$\mathrm{Im}\left(\frac{-1}{\epsilon(k,\omega)}\right)\cong\sqrt{\frac{\pi}{2}}\left(\frac{k}{k_D}\right)^2\left\{\frac{z\ \exp(-z^2/2)}{[1+(k/k_D)^2]^2}\right\}. \tag{A7}$$

Moreover, if $k\gg k_D$, this can be further approximated as:

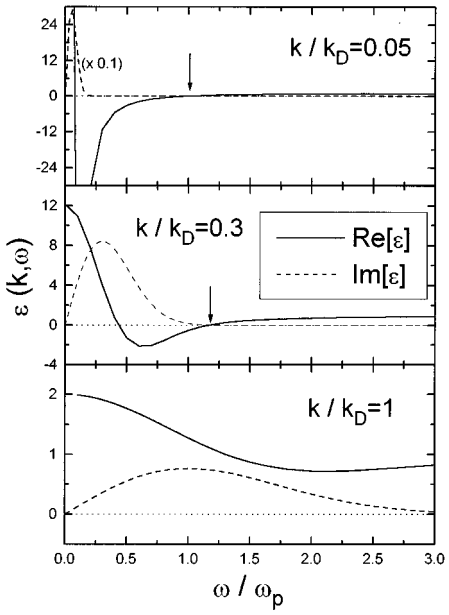

FIG. 11. Behavior of the real and imaginary parts of the dielectric function, vs the frequency ω, for three values of wave vector k: (a) $k/k_D=0.05$, (b) $k/k_D=0.3$, and (c) $k/k_D=1$. In cases (a) and (b) the plasma resonance occurs for $\omega/\omega_P\cong 1$ [when $\mathrm{Re}(\epsilon)=0$ and $\mathrm{Im}(\epsilon)$ is very small] as indicated by the arrows. The real part of ϵ has no zeros at any real frequency for k/k_D values larger than 0.5336; this is illustrated in case (c), for $k/k_D=1$.

$$\mathrm{Im}\left(\frac{-1}{\epsilon(k,\omega)}\right)\cong\sqrt{\frac{\pi}{2}}\frac{(\omega/\omega_P)}{(k/k_D)^3}\exp\left(\frac{-z^2}{2}\right). \tag{A8}$$

3. Dispersion relation for collective modes

Collective longitudinal modes in the plasma exist when

$$\epsilon(k,\omega)=0. \tag{A9}$$

This defines a dispersion relation: $\omega=\omega_r(k)$, which in general yields complex frequencies: $\omega_r(k)=\omega_{r1}(k)+i\omega_{r2}(k)$.

Now, for the collective modes to be well defined, their decay time must be much larger than the characteristic oscillation time, viz.,

$$\left|\frac{\mathrm{Im}[\omega_r(k)]}{\mathrm{Re}[\omega_r(k)]}\right|\equiv\left|\frac{\omega_{r2}(k)}{\omega_{r1}(k)}\right|\ll 1. \tag{A10}$$

The condition $|\omega_{r1}(k)/\omega_{r2}(k)|\sim 0.5$ defines a critical k value for collective modes k_c, such that for $k>k_c$ only individuals modes should be considered.

For a degenerate electron plasma (at $T=0$) there exist the real roots of Eq. (A9) for all values of k smaller than k_c (with $k_c\sim\omega_P/v_F$), and they become complex for $k>k_c$ [17]. In the classical formulation, where Maxwellian-type velocity distributions are introduced, Eq. (A9) has no solutions for real frequencies, and hence plasmons are not sharply defined modes. Nevertheless, Eq. (A6) still remains useful as a first approximation.

A first step to obtain the dispersion relation in Maxwellian plasmas is to assume a very small imaginary component

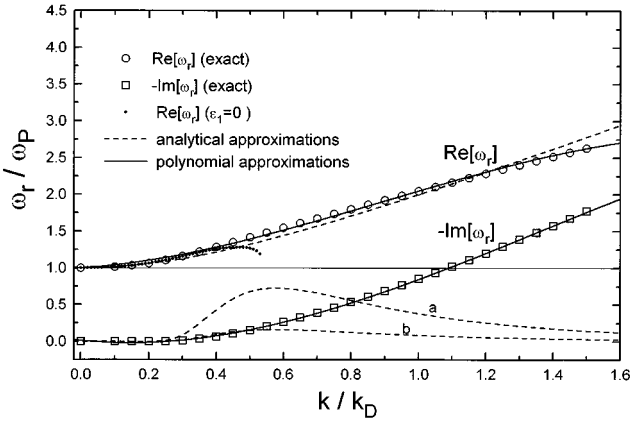

FIG. 12. Determinations of the resonance frequencies vs wave vector k. The roots of Eq. (A9) were numerically evaluated obtaining complex frequencies, shown here by open circles (real part) and squares (imaginary part). The small solid circles are the real roots of $\epsilon_1(k,\omega)=0$. The solid lines show the polynomial approximations to the real and imaginary parts, given by Eq. (A11) with the coefficients of Table II. The dashed lines show the analytical approximations to the real part, given by Eq. (A12), and to the imaginary part, given by Eqs. (A13) (curve labeled a), and (A14) (curve labeled b).

$\epsilon_2\sim 0$ and solve only $\epsilon_1(k,\omega)=0$. This can be readily done for small k ($k<k_D$), such that $z=\omega/kv_T\sim k_D/k$ is large and ϵ_2 becomes very small [cf. Eq. (A5)]. The behavior of $\epsilon_1(k,\omega)$ and $\epsilon_2(k,\omega)$ as a function of ω/ω_P, for fixed values of $k/k_D=0.05$, 0.3, and 1, is shown in Fig. 11. For $k/k_D=0.05$ and 0.3, the plasmon mode is located at $\omega/\omega_P\cong 1$, where in fact $\epsilon_2\sim 0$ and $\epsilon_1=0$. On the contrary, we see that $\epsilon_1(k,\omega)$ has no zeros for $k/k_D=1$ [more precisely, one finds that $\epsilon_1(k,\omega)$ has no real roots for $k/k_D>0.5336$].

More generally, exact solutions of the equation $\epsilon(k,\omega)=0$ were obtained numerically. In this case one finds complex frequencies $\omega_r(k)=\omega_{r1}(k)+i\omega_{r2}(k)$. The results of this procedure are shown in Fig. 12, together with the usual analytical approximations.

For calculation purposes, it become useful to have simple numerical approximations for $\omega_{r1}(k)$ and $\omega_{r2}(k)$. We have obtained polynomial fittings to these solutions, in the form

$$\frac{\omega_r(k)}{\omega_P}=\sum_i a_i\left(\frac{k}{k_D}\right)^i. \tag{A11}$$

The coefficients a_i of these polynomials are given in Table II.

Finally, it is of interest to compare these results with the

TABLE II. Coefficients of the polynomial fittings for the real and imaginary parts of the plasma resonance frequency $\omega_r(k)$ according to Eq. (A11).

	$\mathrm{Re}[\omega_r]$	$\mathrm{Im}[\omega_r]$
a_0	1.0	0.016
a_1	0.3	−0.47
a_2	1.2	1.72
a_3	−0.45	−0.42

analytical approximations to $\omega_r(k)$ obtained from a series expansion of Eq. (A2) for $\omega/k > v_T$, namely, [8,12]

$$\omega_{r1}(k) = \pm\sqrt{1+3(k/k_D)^2}\,\omega_p\,, \tag{A12}$$

$$\omega_{r2}(k) = -\left(\frac{\pi}{8}\right)^{1/2} \frac{\omega_p}{(k/k_D)^3} \exp\left(-\frac{1}{2(k/k_D)^2}\right). \tag{A13}$$

A slightly different approximation for the imaginary part of $\omega_r(k)$ is the following [12]:

$$\omega_{r2}(k) = -\left(\frac{\pi}{8}\right)^{1/2} \frac{\omega_p}{(k/k_D)^3} \exp\left(-\frac{1+3(k/k_D)^2}{2(k/k_D)^2}\right). \tag{A14}$$

These expressions describe the so-called Landau damping of plasma waves [8].

We find from Fig. 12 that the approximation for the real part Eq. (A12) works well in an extended k range (up to $k/k_D \sim 1.5$), whereas Eqs. (A13) and (A14) for the imaginary part deviate rather rapidly from the correct result. Therefore, the polynomial approximation of Eq. (A11) gives, in all cases, a more accurate result.

From these calculations we also find that the ratio $|\omega_{r1}(k)/\omega_{r2}(k)|$ becomes ~ 0.5 for $k/k_D \sim 1.2$. Therefore, we can conclude that the usual cutoff for the collective modes at $k_c \sim k_D$, may be used as a good approximation to separate the regimes of collective and individual excitations in the evaluation of the stopping terms.

[1] E. Speth, Rep. Prog. Phys. **52**, 57 (1989).
[2] C. Deutsch, Laser Part. Beams **8**, 541 (1990); C. Deutsch and N. A. Tahir, Phys. Fluids B **4**, 3735 (1992).
[3] E. Nardi, Z. Zinamon, and D. Ben-Hamu, Nuovo Cimento A **106**, 1839 (1993).
[4] N. R. Arista, Phys. Rev. B **18**, 1 (1978).
[5] G. Basbas and R. H. Ritchie, Phys. Rev. A **25**, 1943 (1982).
[6] D. Bohm and D. Pines, Phys. Rev. **85**, 338 (1952).
[7] D. Pines, J. Nucl. Energy Part C **2**, 5 (1961).
[8] J. Ichimaru, *Basic Principles of Plasma Physics* (Benjamin, New York, 1973).
[9] L. de Ferrariis and N. R. Arista, Phys. Rev. A **29**, 2145 (1984).
[10] N. R. Arista and W. Brandt, Phys. Rev. A **30**, 630 (1984).
[11] P. M. Echenique, R. H. Ritchie, and W. Brandt, Phys. Rev. B **20**, 2567 (1979).
[12] T. Peter and J. Meyer-ter-Vehn, Phys. Rev. A **43**, 1998 (1992).
[13] L. Spitzer, *Physics of Fully Ionized Gases* (Wiley, New York, 1963); S. T. Butler and M. J. Buckingham, Phys. Rev. **126**, 1 (1962).
[14] N. R. Arista and W. Brandt, Phys. Rev. A **23**, 1898 (1981); **29**, 1471 (1984).
[15] G. Maynard and C. Deutsch, J. Phys. (Paris) **46**, 1113 (1985).
[16] A. Bret and C. Deutsch, Phys. Rev. E **47**, 1276 (1993).
[17] D. Pines, *Elementary Excitations in Solids* (Benjamin, New York, 1964); P. M. Platzman and P. A. Wolff, in *Waves and Interactions in Solid State Plasmas*, Vol. 13 of Solid State Physics (Academic, New York, 1973).
[18] J. D'Avanzo, M. Lontano, and P. F. Bortignon, Phys. Rev. A **45**, 6126 (1992).
[19] J. D'Avanzo, M. Lontano, and P. F. Bortignon, Phys. Rev. E **47**, 3574 (1993).
[20] *Handbook of Mathematical Functions*, edited by M. Abramowitz and I. Stegun (Dover, New York, 1972).
[21] E. M. Bringa and N. R. Arista, Phys. Rev. E **52**, 3010 (1995).